The Journal of Chemical Physics

Pulse propagation and oscillatory behavior in the NO+H_2 reaction on a Rh(110) surface

Cite as: J. Chem. Phys. **105**, 4317 (1996); https://doi.org/10.1063/1.472248
Submitted: 03 January 1996 • Accepted: 30 April 1996 • Published Online: 31 August 1998

F. Mertens and R. Imbihl

View Online Export Citation

ARTICLES YOU MAY BE INTERESTED IN

Reaction diffusion patterns in the catalytic CO-oxidation on Pt(110): Front propagation and spiral waves
The Journal of Chemical Physics **98**, 9977 (1993); https://doi.org/10.1063/1.464323

Simulations of the NO+NH_3 and NO+H_2 reactions on Pt(100): Steady state and oscillatory kinetics
The Journal of Chemical Physics **98**, 5526 (1993); https://doi.org/10.1063/1.464900

Breakdown of global coupling in oscillatory chemical reactions
The Journal of Chemical Physics **99**, 8668 (1993); https://doi.org/10.1063/1.465590

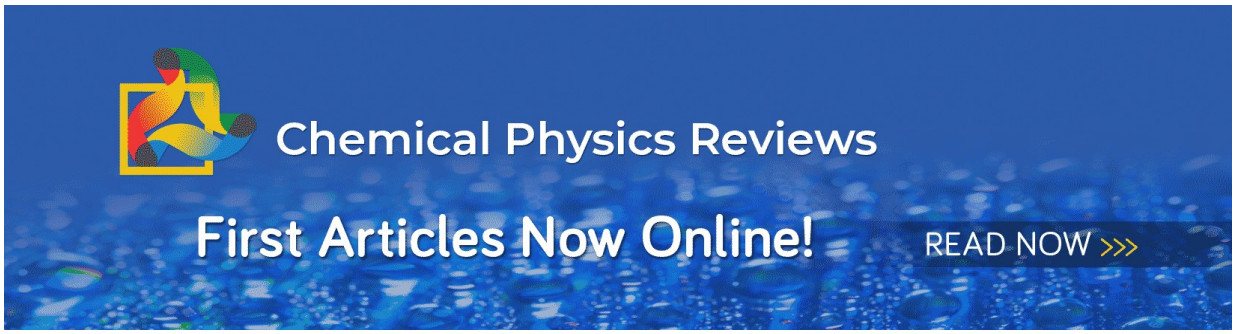

AIP Publishing

© 1996 American Institute of Physics.

Pulse propagation and oscillatory behavior in the $NO+H_2$ reaction on a Rh(110) surface

F. Mertens[a)]
Fritz-Haber-Institut der Max-Planck-Gesellschaft, Faradayweg 4-6, D-14195 Berlin, Germany

R. Imbihl
Institut für Physikalische Chemie und Elektrochemie, Universität Hannover, Callinstr. 3-3a, D-30167 Hannover, Germany

(Received 3 January 1996; accepted 30 April 1996)

Target patterns, rotating spiral waves and solitary pulses have been found in the $NO+H_2$ reaction under nonoscillatory conditions, i.e., when the system was an excitable medium. Using photoelectron emission microscopy (PEEM) as spatially resolving method the parameter dependence of the front velocities, the width of the pulses and the rotational period of the spiral waves were studied for fixed $p_{NO}=1.8\times10^{-6}$ mbar in a T- range 520–620 K. The front velocities were strongly anisotropic with the degree of anisotropy depending on the p_{H_2}, T parameters. Under reaction conditions close to the high p_{H_2} boundary for pattern formation, gas-phase coupling becomes efficient, thus, oscillations in the N_2 production rate can be observed. © *1996 American Institute of Physics.* [S0021-9606(96)01230-5]

I. INTRODUCTION

Spatiotemporal pattern formation on single crystal surfaces has been studied under well-defined low pressure conditions ($p<10^{-3}$ mbar) for a number of reactions involving catalytic CO oxidation and catalytic NO reduction.[1–3] Although mathematical models for chemical waves in isotropic media can be easily formulated for simple activator-inhibitor systems, the development of a realistic model for a surface reaction is a much more difficult task. One of the principle difficulties one faces in the simulations is to take surface diffusion of adsorbed particles properly into account since adsorbate–adsorbate interactions and adsorbate-induced reconstructions will make both, the magnitude of the diffusion coefficient as well as the anisotropy coverage dependent.[4,5]

One system which, on one hand, is rather complex with respect to the mechanism, but, on the other hand, offers a particularly rich variety of chemical wave patterns is catalytic NO reduction with H_2 on Rh(110). In this system, besides the usual elliptically shaped wave patterns, rectangularly shaped target patterns and traveling wave fragments have been found.[6–8] The unusual shape of the wave patterns has been attributed to a state-dependent anisotropy of surface diffusion caused by the presence of different types of adsorbate-induced reconstructions in this system.[7,9] The existence range for chemical wave patterns has been mapped out in parameter space and *in situ* low energy electron diffraction (LEED) experiments verified the existence of different reconstruction geometries under reaction conditions.[10]

Although simulations based on a general model could reproduce qualitatively the observed effects, no detailed mechanistic model and, hence, no realistic mathematical model has yet been developed.[7–9] The aim of this investigation was to study the parameter dependence and the anisotropy of front propagation quantitatively in order to be able to develop such a realistic model. In the course of this investigation, it was also discovered that by choosing certain reaction parameters, the system which usually under the conditions of pattern formation exhibits a stationary reaction rate can turn into an oscillatory system displaying sustained rate oscillations. This transition is attributed to gas-phase coupling causing synchronization of the reacting surface.

II. EXPERIMENT

The experiments have been conducted in a standard UHV system (ca. 80 l vol) which under reaction conditions was operated as a continuous flow reactor (effective pumping rate ≈100 l/s). The system was equipped with LEED, an Auger electron spectrometer, a differentially pumped quadrupole mass spectrometer (QMS), and a photoelectron emission microscope (PEEM) as spatially resolving method. PEEM which is sensitive to local work function variations allows one to image the reacting surface with a lateral resolution of ≈1 μm and the temporal resolution of video frames (50 ms).[11] The Rh(110) single crystal (diam ≈7 mm) which was polished with diamond paste down to 0.03 μm was the same as used in previous experiments.[7,8] Before measurements, the crystal surface was cleaned by a combination of Ar ion sputtering at 800 K (2 kV, 2.5 μA, 30–45 min), annealing to 1470 K, oxygen treatment at 1070 K ($p_{O_2}=1\times10^{-6}$ mbar, 5 min) followed by a second annealing to 1470 K. Gases (purity H_2 5.3, NO 2.5) were introduced via leak valves. A feedback-stabilized gas inlet system ensured that the partial pressures could be kept constant within <0.5%. All partial pressures given in this report have been corrected by the relative ionization probabilities S/S_{N_2} being 0.45 for H_2 and 1.2 for NO.

[a)]Present address: Center for Nonlinear Dynamics, University of Texas, Austin, Texas 78712.

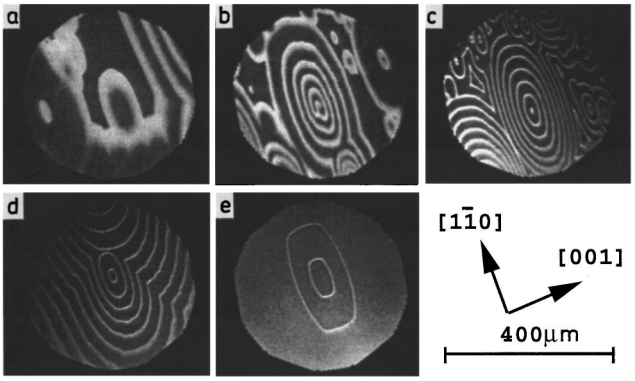

FIG. 1. PEEM images demonstrating changes in width of traveling pulses as p_{H_2} is varied with p_{NO} and T being kept constant at $T=560$ K and $p_{NO}=1.8\times10^{-6}$ mbar. p_{H_2} in [10^{-5} mbar]: 1.76 (a), 1.67 (b), 1.25 (c), 0.9 (d), 0.5 (e).

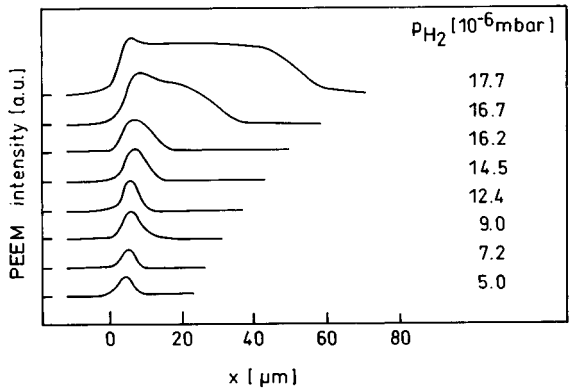

FIG. 2. PEEM intensity profiles showing the changes in the shape and in the width of an individual pulse as p_{H_2} is varied. The profiles were taken along the [110] direction from the PEEM images displayed in Fig. 1. They show chemical waves moving from right to left.

III. RESULTS

A. Chemical wave patterns

Chemical wave patterns were initiated in a typical procedure by first raising p_{H_2} up to 1×10^{-4} mbar which caused the whole area imaged in PEEM to become uniformly white. p_{H_2} was then rapidly decreased to a fixed value. This first transformed the imaged surface into a uniformly dark area, after a waiting period of $\approx$10–30 s, before white bands started to nucleate at some defects and spread out. Examples of the target patterns which are formed in this way are displayed in Fig. 1. The white area in these images corresponding to a low work function has been assigned to the bare or nitrogen covered surface while the dark area representing a high work function has been associated with a predominantly oxygen covered surface. The patterns are anisotropic with the long axis oriented in the [110] direction and it was shown before that the shape and the anisotropy of the wave patterns vary with the experimental parameters.[6,8,10] The moving white bands in the PEEM images represent traveling pulses in an excitable medium and in the following the parameter dependence of the shape and the velocity of the pulses is investigated.

As demonstrated by the PEEM images in Fig. 1, with increasing hydrogen partial pressure, the width and the brightness of the traveling pulses increase quite strongly. Profile cuts through the PEEM images displayed in Fig. 2 show that first the effect of a p_{H_2} increase is relatively small, but above a certain threshold which for the chosen p_{NO}, T conditions lies around 1.6×10^{-5} mbar, the width and the height of the pulses grow drastically with p_{H_2}. In addition, one notes that at the highest p_{H_2} the profiles develop a plateau and a shoulder at the leading edge.

With increasing p_{H_2} the pulse velocity, v, increases but as a consequence of the anisotropy of the surface, the pulse velocity is strongly anisotropic. This is illustrated by Fig. 3 showing the dependence of the pulse velocity on p_{H_2} for the two main crystallographic directions of Rh(110). In order to avoid dispersion effects which would have distorted the dependence of v on experimental parameters, the velocity v was measured here and in the following diagrams always at a sufficiently large wavelength, i.e., under conditions where subsequent pulses do not interact. As expected from the geometry of the unreconstructed surface the fronts advance more rapidly in the [110] direction, i.e., along the direction of the (110) troughs than perpendicular to the troughs.

Furthermore, one notes that the front velocity along the [001]-direction exhibits only a small dependence on p_{H_2} while the velocity along [1$\bar{1}$0], $v_{[1\bar{1}0]}$ increases steeply with p_{H_2}. We define as a measure, p, for the anisotropy of front propagation, simply, the ratio of the velocities along the crystallographic directions, $v_{[1\bar{1}0]}/v_{[001]}$, with $p=1$ representing the isotropic case. Figure 3 then evidently demonstrates that the anisotropy is not constant but depends on the experimental parameters.

The dependence of the pulse velocity on the temperature is shown in Fig. 4 for the two main crystallographic directions. Qualitatively the dependence on temperature looks

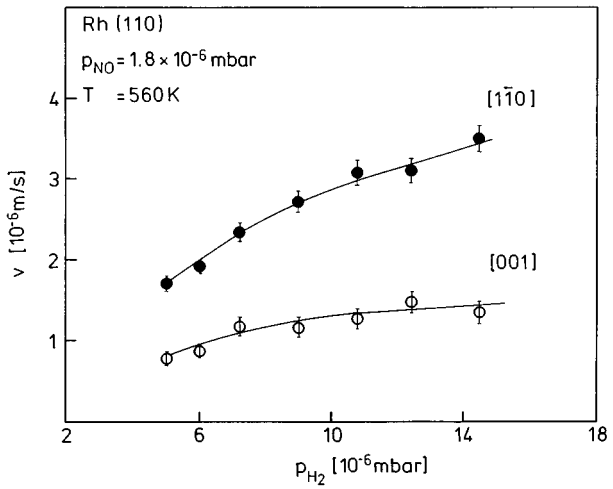

FIG. 3. Dependence of the pulse velocity, v, on p_{H_2} for the two main crystallographic directions of Rh(110).

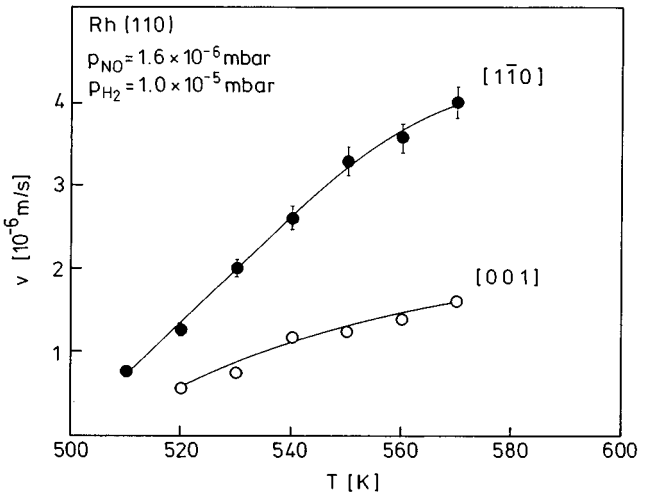

FIG. 4. Dependence of the pulse velocity, v, on temperature for the two main crystallographic directions of Rh(110).

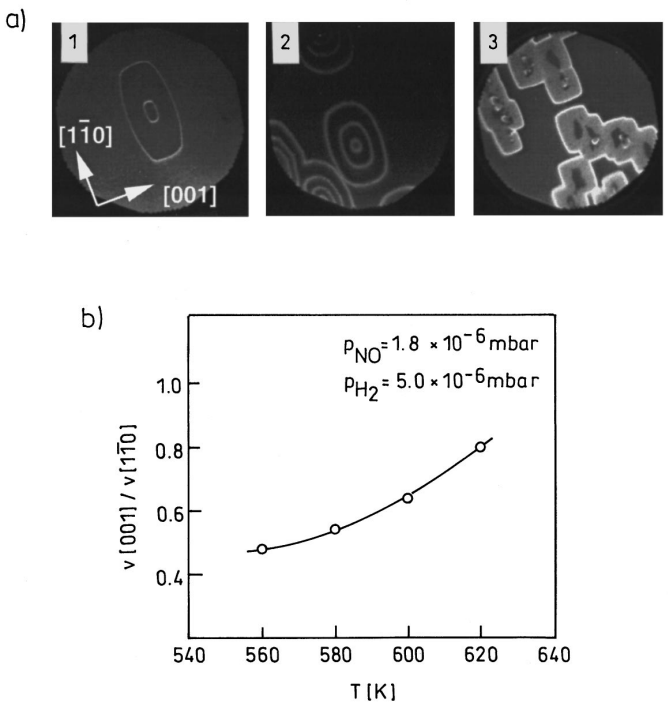

FIG. 5. Influence of temperature on the shape of the chemical wave patterns in a parameter range where rectangularly shaped patterns can be found (a) PEEM images showing target patterns at different temperatures. Experimental conditions: frame No. 1, T=560 K, p_{NO}=1.8×10^{-6} mbar, p_{H_2}=5.0×10^{-6} mbar; frame No. 2, T=600 K, p_{NO}=1.6×10^{-6} mbar, p_{H_2}=6.9×10^{-6} mbar; frame No. 3, T=620 K, p_{NO}=1.8×10^{-6} mbar, p_{H_2}=5.0×10^{-6} mbar. The diameter of the imaged area is 400 μm for frames Nos. 1 and 3 and 470 μm for frame No. 2. (b) Dependence of the anisotropy of front propagation on temperature in a parameter range where rectangularly shaped patterns are observed.

rather similar to the one on p_{H_2} but in contrast to the p_{H_2} dependence the ratio $v_{[1\bar{1}0]}/v_{[001]}$ almost does not change with temperature, i.e., the anistoropy remains constant. The qualitative picture which results from Fig. 4 is, however, only correct if p_{H_2} is sufficiently large. If one investigates the T dependence of v under conditions of low p_{H_2} and higher temperature, i.e., when rectangularly shaped target patterns are seen, the dependence displayed in Fig. 5(b) is observed. Here, the anisotropy approaches 1 at the high T boundary for pattern formation. The corresponding PEEM images which are reproduced in Fig. 5(a) demonstrate that the change in anisotropy corresponds to a transition from rectangular patterns at low T to almost square-shaped target patterns at high T.

Pulses in catalytic surface reactions are typically triggered by structural defects.[1,2] If these trigger centers have strongly different firing frequencies, one obtains PEEM images like the one reproduced in Fig. 6 showing a target pattern with a high firing frequency on the right half and several target patterns with low firing frequencies on the left half. Due to annihilation of colliding wave fronts the target pattern with the high firing frequency will finally displace the other target patterns. In Fig. 6, the waves which are created by the fast firing trigger center (right half) propagate much slower than the waves initiated by the low-frequency trigger centers. The corresponding dispersion relation is displayed in Fig. 7 for the two main crystallographic directions. The diagram more or less reflects the fact that a slowing down results if the wavelength of the patterns becomes so small that each pulse runs into the refractory tail of the preceding pulse. In Fig. 7, both directions exhibit similar dispersion behavior but the curve for the [110] direction is clearly shifted to larger wavelengths as compared to the [001] curve.

In the NO+H_2 reaction on Rh(110) target patterns were the dominant type of wave patterns and rotating spiral waves were only rarely seen.[6,7] In areas with a large number of structural defects, many spirals could be observed, but these spirals which were pinned to structural defects could usually not develop more than two to three windings. Well-developed spirals could, in some cases, be initiated in a parameter range in which the chemical wave patterns exhibited a rectangular shape.[7] An example of such a rectangular spiral wave is displayed in Fig. 8(a). For such spirals the dependence of the rotational frequency on p_{H_2} was investigated

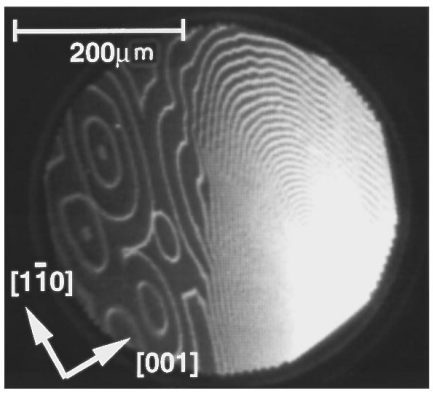

FIG. 6. Displacement of a target patterns with low firing frequencies by a target pattern with a high firing frequency. Experimental conditions: T=560 K, p_{NO}=1.8×10^{-6} mbar, p_{H_2}≈1×10^{-5} bar.

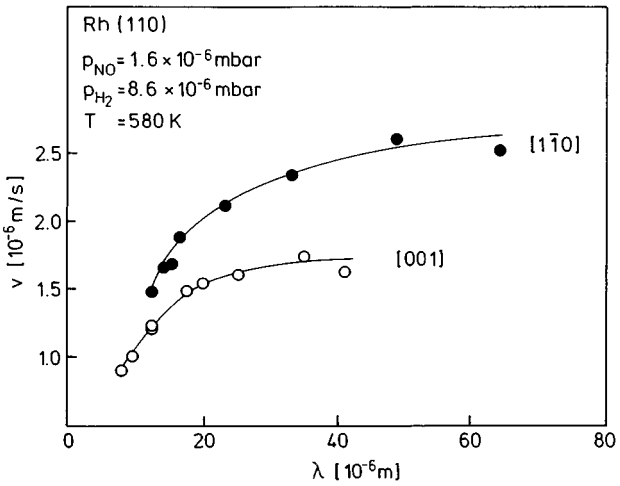

FIG. 7. Dispersion relation for pulse propagation along the two main crystallographic directions of Rh(110).

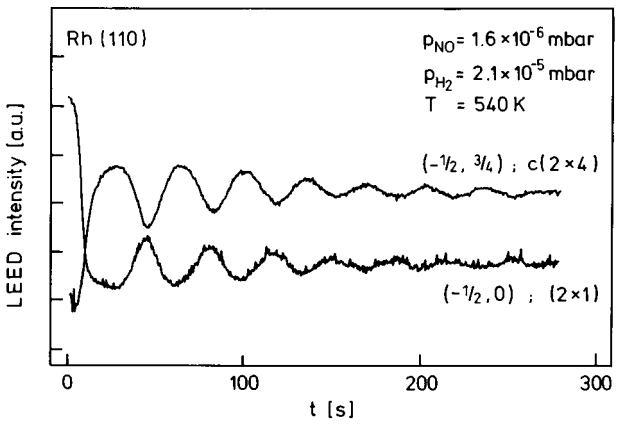

FIG. 9. Damped oscillations in the LEED intensities of the $c(2\times4)$-N,O and the (2×1)-N structure initiated by a sharp p_{H_2} decrease from 1×10^{-4} mbar to 2.1×10^{-5} mbar.

and the results are reproduced in Fig. 8(b). For low p_{H_2}, the rotational frequency increases roughly linearly with p_{H_2} until the frequency starts to level off at $p_{H_2}\sim8\times10^{-6}$ mbar.

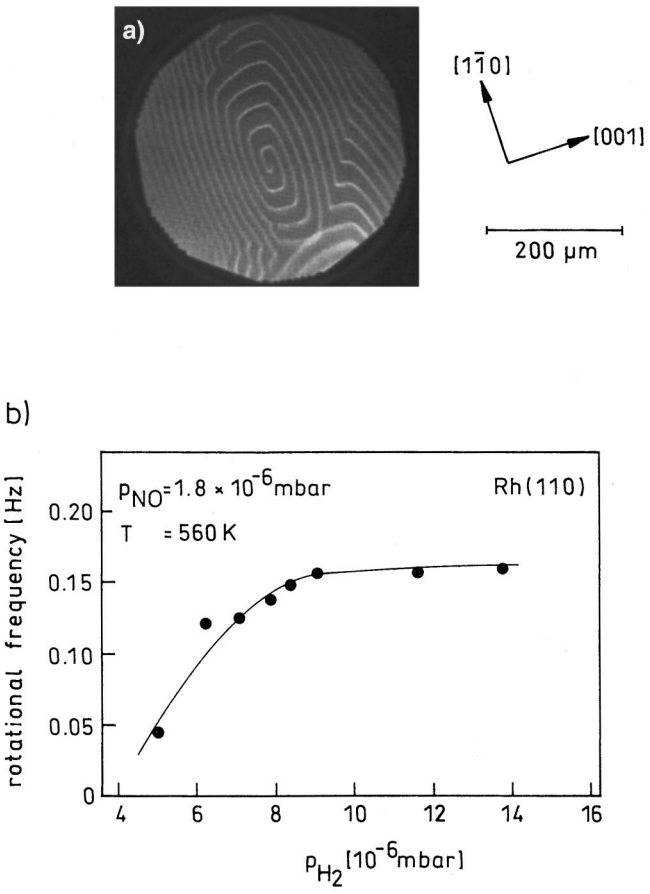

FIG. 8. Dependence of the rotational frequency of a rectangularly shaped spiral wave on p_{H_2}. (a) PEEM image of a rectangular spiral wave. Experimental conditions: T=560 K, $p_{NO}=1.8\times10^{-6}$ mbar, $p_{H_2}=5.0\times10^{-6}$ mbar. (b) Dependence of the rotational frequency of spiral waves on p_{H_2}.

B. Rate oscillations

Rate oscillations can occur in a pattern forming surface reaction if either the length scale of the patterns is comparable to the dimensions of the surface or if a global coupling mode is present which synchronizes the local oscillators at different parts of the surface.[1,2] A global coupling mode is provided by the small partial pressure variations of the educts which arise in an oscillatory system due to mass balance in the reaction. This mode can become effective if the surface reaction is sensitive enough to small amplitude variations of the educt partial pressures.

If reaction conditions are chosen which are well inside the parameter range for pattern formation in the Rh(110)/NO+H_2 system, no rate oscillations can be observed. Only damped oscillations can be initiated by a sudden synchronizing parameter change but these oscillations die away within a small number of cycles as demonstrated by the LEED intensity oscillations displayed in Fig. 9. If, however, reaction conditions are adjusted close to the high p_{H_2} boundary for pattern formation, then sustained rate oscillations develop. The oscillations in the N_2 production rate and the concomitant small changes in p_{NO} which are responsible for synchronizing the surface reaction are displayed in Fig. 10.

At points marked by arrows in Fig. 10, PEEM images were taken showing at which stages in the pattern forming process synchronization occurs. The PEEM images displayed in Fig. 11 demonstrate that the sharp rise in the reaction rate in Fig. 10 is associated with the development of a target pattern which then is extinguished at the rate maximum. The fast time scale in these relaxation-type oscillations is, therefore, connected with a transition via pattern formation which transforms the homogeneously dark area [Fig. 11(a)] to a homogeneously white area [Fig. 11(f)]. A slow relaxation process then leads back from the white area [Fig. 11(f)] to the dark area [Fig. 11(i)]. In contrast to the fast rise of the reaction rate, the relaxation process is not associated with pattern formation. The remaining weakly visible pat-

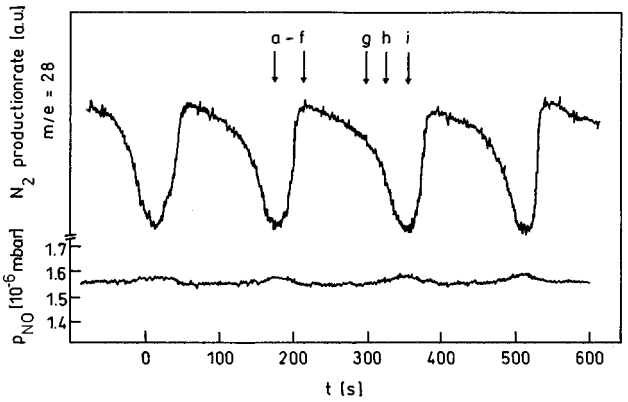

FIG. 10. Sustained oscillations in the N_2 production rate observed at $T=550$ K, $p_{NO}=1.6\times10^{-6}$ mbar, $p_{H_2}=2.0\times10^{-5}$ mbar. The diagram also displays the variations in p_{NO} which arise due to mass balance in the reaction system. The arrows denote the time moments where the PEEM images shown in Fig. 11 were taken from the reacting surface.

terns which are seen in Figs. 11(f) and 11(g) are not dynamic and can be attributed to a memory effect of the surface, i.e., they are reminiscence of the patterns formed in steps a–e. These patterns are probably caused by structural changes of the surface which were not completely removed in the subsequent development.

The positive feedback which has to exist between the partial pressure variations and the surface reaction in order to allow for synchronization can be constructed in a very simple way. First, it is important to note that an increase in the reaction rate will lead to a decrease of both, p_{NO} and p_{H_2}. Since, however, hydrogen is in excess by about one order of magnitude, the relative variation in p_{H_2} is small and it is sufficient to consider the changes in p_{NO} solely.

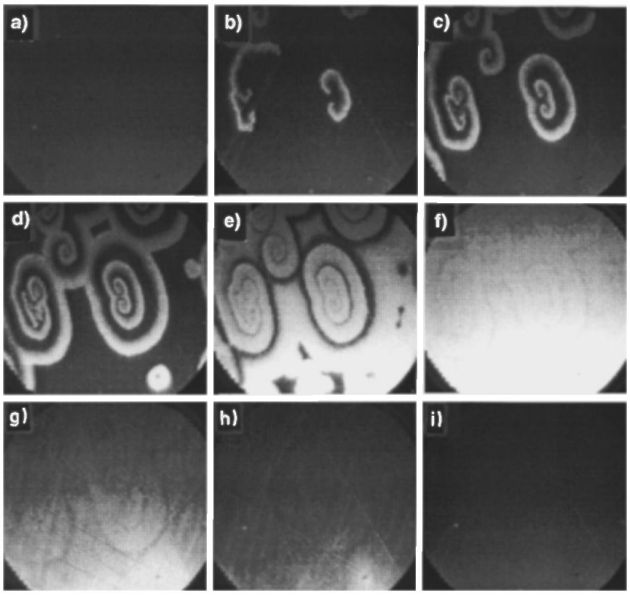

FIG. 11. PEEM images showing the development of patterns and the influence of gas-phase coupling during rate oscillations. The images were taken at the points marked by arrows in Fig. 10.

The data in Figs. 10 and 11 demonstrate that the rate minimum is associated with a uniform dark area corresponding to an oxygen covered surface whereas the uniform bright area at the rate maximum can be associated with a nitrogen covered/bare Rh(110) surface.[10] Starting with the unreactive surface at Fig. 11(a), the spreading of the white bands will cause the reaction rate to increase and consequently the ratio p_{NO}/p_{H_2} will become smaller. This leads to increase in the front velocity (see Fig. 3) and, furthermore, it initiates the nucleation of waves as can be seen clearly in Fig. 11(d). Hence, the reactive area will grow and the concomitant further decrease of p_{NO}/p_{H_2} establishes the positive feedback which leads to a rapid transformation of the whole surface.

IV. DISCUSSION

A. Pattern formation

Front propagation in the $NO+H_2$ reaction on Rh surfaces has been investigated in several field electron microscopy (FEM) studies by Nieuwenhuys *et al.*.[12,13] In FEM very regular spatiotemporal patterns with near atomically sharp interfaces were observed which reflect the different reactivities of the various orientations on the Rh field emitter tip. So far, for the FEM experiments or for the chemical waves in $Rh(110)/NO+H_2$ an experimentally proven oscillation/excitation mechanism does not exist. For the latter system, a large number of single crystal studies have been conducted focusing on the adsorbate-induced reconstructions which occur under the influence of adsorbates such as oxygen and nitrogen.[14–18] These studies essentially demonstrate that the system Rh(110)/N,O exhibits an enormous structural variability and, consequently, it is rather difficult to understand the detailed interplay between the surface reaction and adsorbate-induced substrate changes.

Although the excitation mechanism for the pulses in $Rh(110)/NO+H_2$ has not yet been established, there is little doubt that the cause for the formation of the primary reaction front lies in the inhibitory effect of a dense oxygen adlayer on hydrogen adsorption.[19] The mechanism explaining the formation of the primary front, i.e., the leading front in a pulse, can be sketched as follows. Starting with a fully oxygen covered surface the adsorption of hydrogen will be completely blocked except at some structural defects. Hydrogen adsorbing at these defects will diffuse to neighboring sites, react with oxygen thus creating vacant sites. These sites will allow more hydrogen to adsorb and react leading to an autocatalytic increase in the number of vacant sites. The autocatalytic reaction in connection with the diffusion of atomic hydrogen, therefore, creates a propagating reaction front similar to the mechanism which is causing a reaction front in the reactive removal of a CO adlayer in catalytic CO oxidation.[1,2]

It has already been outlined before that the presence of adsorbate-induced reconstructions with different substrate geometries leads to a state-dependent diffusional anisotropy.[6–8] Such a complex anisotropy explains in principle the origin of the rectangularly shaped patterns but it remains of course to be shown what the actual values of the

diffusion constants are, to what degree the anisotropy is determined by the geometric surface corrugation, and what role adsorbate–adsorbate interactions play.

B. Rate oscillations

Rate oscillations in the catalytic reduction of NO with hydrogen have been observed under low pressure conditions ($p<10^{-3}$ mbar) on Pt(100), Rh(110), and on Rh(533).[20–24] Rate oscillations in the $NO+H_2$ reaction on Rh(110) have recently been found by Kruse *et al.*, but these oscillations occur at much higher temperature, at ≈900 K, than the oscillations presented here.[24] For this reason, it is very likely that a different mechanism is operating in the high temperature oscillations. In the oscillation studies periodic variations in the production rate of N_2, NH_3, and N_2O have been detected. For the oscillations on Pt(100) a detailed mathematical model for the oscillations has been proposed based upon the vacancy mechanism for NO dissociation.[22] For the oscillations on Rh surfaces, no detailed mechanism has been suggested so far although the comparison of the oscillatory T range with N_2 thermal desorption data clearly indicates that the stability of the nitrogen adlayer has to play an essential role in the mechanism.

In contrast to other oscillatory reactions on single crystal surfaces, the oscillatory parameter range in the system $Rh(110)/NO+H_2$ is only a very small subset of the existence range for pattern formation. This relation is a consequence of the fact that gas-phase coupling only becomes effective near the high p_{H_2} boundary for pattern formation. The synchronizing effect gas-phase of coupling can be traced back to a positive feedback between the spreading of the reactive zone and the concomitant variations in p_{NO}. The efficiency of gas-phase coupling is, of course, limited by the sensitivity of the surface reaction to partial pressure changes, the experimental parameters like flow rate and chamber volume which determine the magnitude of these changes, and inhomogeneities of the sample surface. The narrowness of the existence range for rate oscillations might, therefore, be strongly dependent on experimental parameters.

The rate oscillations depicted in Fig. 10 are relaxation-type oscillations and the comparison with the PEEM images in Fig. 11 reveals that we can assign different surface processes to the two time scales. The fast time scale can be associated with a pattern formation and synchronization process while the interpretation of the slow deactivation process which proceeds spatially uniformly is not quite clear. It could be caused by the formation or removal of a subsurface oxygen species or be due to some other strongly activated process. Evidence for subsurface oxygen formation has been presented for Rh(210) and Rh(110) but the involvement of this species into the oscillations in $Rh(110)/NO+H_2$ remains to be shown.[25,26]

V. CONCLUSIONS

The system $Rh(110)/NO+H_2$ behaves as an excitable medium in almost the entire parameter range for pattern formation and only close to the high p_{H_2} boundary of this existence range can oscillations in the reaction rate be observed. Pulse propagation in this system is strongly anisotropic, but the anisotropy is not constant but depends on the experimental parameters. Pulse propagation exhibits the characteristic features of an excitable medium as evidenced by a strong dispersion of the front velocity vs the wavelength. Rate oscillations of the relaxation-type have been observed in the N_2 production. The rate oscillations arise under conditions when gas-phase coupling becomes effective leading to a synchronization of the reacting surface.

ACKNOWLEDGMENT

The authors are thankful to S. Wasle for preparation of the drawings.

[1] G. Ertl, Science **254**, 1750 (1991).
[2] R. Imbihl, Prog. Surf. Sci. **44**, 185 (1993).
[3] R. Imbihl and G. Ertl, Chem. Rev. **95**, 697 (1995).
[4] S. J. Lombardo and A. T. Bell, Surf. Sci. Rep. **13**, 1 (1991).
[5] A. Mikhailov and G. Ertl, Chem. Phys. Lett. **238**, 104 (1995).
[6] F. Mertens and R. Imbihl, Nature **370**, 124 (1994).
[7] N. Gottschalk, F. Mertens, M. Bär, M. Eiswirth, and R. Imbihl, Phys. Rev. Lett. **73**, 3483 (1994).
[8] F. Mertens, N. Gottschalk, M. Bär, M. Eiswirth, A. Mikhailov, and R. Imbihl, Phys. Rev. E **51**, R5196 (1995).
[9] A. Mikhailov, Phys. Rev. E **49**, 5875 (1994).
[10] F. Mertens and R. Imbihl, Surf. Sci. **347**, 355 (1996).
[11] W. Engel, M. E. Kordesch, H. H. Rotermund, S. Kubala, and A. von Oertzen, Ultramicroscopy **36**, 148 (1991).
[12] M. F. H. van Tol, A. Gielbert, and B. E. Nieuwenhuys, Appl. Surf. Sci. **67**, 179 (1993); Catal. Lett. **16**, 297 (1992).
[13] A. R. Cholach, M. F. H. van Tol, and B. E. Nieuwenhuys, Surf. Sci. **320**, 281 (1994).
[14] F. M. Leibsle, P. W. Murray, S. M. Francis, G. Thornton, and M. Bowker, Nature **363**, 706 (1993).
[15] M. Kiskinova, S. Lizzit, G. Comelli, G. Paolucci, and R. Rosei, Appl. Surf. Sci. **64**, 183 (1993).
[16] V. R. Dhanak, A. Baraldi, R. Rosei, M. Kiskinova, P. W. Murray, G. Thornton, and M. Bowker, Phys. Rev. B **50**, 8807 (1994).
[17] P. W. Murray, G. Thornton, M. Bowker, V. R. Dhanak, A. Baraldi, and M. Kiskinova, Phys. Rev. Lett. **71**, 4369 (1993).
[18] M. Gierer, F. Mertens, H. Over, G. Ertl, and R. Imbihl, Surf. Sci. **339**, L903 (1995).
[19] F. Mertens and R. Imbihl, Chem. Phys. Lett. **242**, 221 (1995).
[20] M. Slinko, T. Fink, T. Löher, H. H. Madden, S. J. Lombardo, R. Imbihl, and G. Ertl, Surf. Sci. **264**, 157 (1992).
[21] J. Siera, P. Cobden, K. Tanaka, and B. E. Nieuwenhuys, Catal. Lett. **10**, 335 (1991).
[22] S. J. Lombardo, T. Fink, and R. Imbihl, J. Chem. Phys. **98**, 5526 (1993).
[23] N. M. H. Janssen, B. E. Nieuwenhuys, M. Ihai, K. Tanaka, and A. R. Cholach, Surf. Sci. **319**, L29 (1994).
[24] S. Heinze, V. Schmatloch, and N. Kruse, Surf. Sci. **341**, 124 (1995).
[25] M. Rebholz, P. Prins, and N. Kruse, Surf. Sci. **269/270**, 293 (1992).
[26] V. Schmatloch, I. Jirka, S. Heinze, and N. Kruse, Surf. Sci. **331–333**, 23 (1995).